Structure and Thermodynamics of $NaF-AlF_3$ Melts with Addition of CaF_2 and MgF_2

Bernard Gilbert,[†] Eric Robert,[†] Eric Tixhon,[†] Jørn E. Olsen,[‡] and Terje Østvold*[,‡]

Laboratoire de Chimie Analytique, Université de Liège, B-4000 Liège, Belgium, and Institute of Inorganic Chemistry, Norwegian University of Science and Technology, N-7034 Trondheim, Norway

Received December 28, 1995[⊗]

The $NaF-AlF_3$ system with additions of CaF_2 and MgF_2 has been studied with Raman and vapor pressure measurements for $3 \geq CR$ (NaF/AlF_3 molar ratio) ≥ 1 and up to 50 mol % additive. The results show that the binary melt can be described using the two equilibria $AlF_6^{3-} = AlF_6^{2-} + F^-$ and $AlF_5^{2-} = AlF_4^- + F^-$ with equilibrium constants 0.25 and 0.05, respectively, at 1293 K. Both reactions have positive reaction enthalpies. The first equilibrium is strongly shifted to the right resulting in a melt mixture with very low AlF_6^{3-} concentrations even at the Na_3AlF_6 composition. Evidence for nonideal mixing of anions was found. For the ternaries, models based on Raman data are presented and compared with vapor pressure measurements. Good agreement is observed when association between the additives, CaF_2 or MgF_2, with the AlF_5^{2-} ions in the melt was considered. This association could be experimentally observed through a band broadening and a slight shift in the AlF_5^{2-} band frequency. Our vapor pressures and Raman data both indicate that MgF_2 clearly acts as an acid when added to $NaF-AlF_3$ melts of any composition. When CaF_2 is added, a slight decrease of vapor pressure occurs. Raman data indicate a decrease of AlF_4^- concentration, corresponding to a dissociation of CaF_2 with liberation of F^- ions. All these results are, however, very much dependent on the initial melt composition. These data are explained in terms of acid−base, dilution, and association reactions of the solute with the solvent.

Introduction

Owing to their industrial interest, cryolite-based melts have been studied intensively over many years to obtain useful data for the aluminium industry. It has, however, not been possible to obtain a structural model consistent with all the experimental data available. Raman spectroscopy provides a powerful tool to obtain the molten salt structure at the molecular level. The development of windowless cells to handle corrosive fluorides and new techniques to obtain quantitative information on the concentration of ionic complexes present in such melts[1] give a new possibility to study these technically important liquids. When Raman spectroscopy is used in combination with techniques that give thermodynamic data, we have a much better basis for a discussion of the connection between structure, thermodynamics, and possible models for these liquid systems.

In technical aluminium electrolysis, the acid−base concept is used to describe the excess AlF_3 content in cryolitic melts. Although this is not strictly correct, however, an acidic electrolyte is conventionally considered to be a melt with AlF_3 in excess over the Na_3AlF_6 composition and a basic electrolyte is a melt where there is an excess of NaF. Cryolite is considered to dissociate in the liquid state to AlF_4^- and F^- ions where AlF_4^- is the acidic component and F^- the base. This concept must be taken with care, since it may lead to misunderstandings. In this paper, we will discuss acid−base properties based on our experimental data and the work of Dewing.[2] We made some misleading interpretations of our data concerning the acid−base properties of CaF_2 in a previous paper.[3] These interpretations have now been corrected.

Several authors have presented activity data for Na_3AlF_6 and $NaAlF_4$ in $NaF-AlF_3$ melts.[4−9] The most consistent and reliable discussion seems to be the one presented by Dewing,[5] who used calorimetric data, vapor pressure data, the sodium content of aluminium in equilibrium with $NaF-AlF_3$ melts, and data from emf measurements to obtain activities. Sterten and Mæland[6] have published a paper where activities in cryolitic melts are discussed. The calculated activities do, however, seem to contain some minor inconsistencies.[3]

No direct evidence for the presence of the AlF_4^- and AlF_6^{3-} ions in these melts was demonstrated before Gilbert *et al.*[10] presented Raman spectra of liquid $NaF-AlF_3$ melts. New results obtained from a study involving a much larger composition range indicated also that a new species assumed to be AlF_5^{2-} was present.[11] Such an ion had also been predicted by Dewing[12] based on thermodynamic arguments. Further Raman work by Gilbert *et al.* on the $NaF-AlF_3-CaF_2$[13] and the $KF-AlF_3$[14] liquid systems strengthen the hypothesis of the formation of three ionic complexes AlF_4^-, AlF_5^{2-}, and AlF_6^{3-} in these melts.

In technical electrolysis of aluminium, the base melt $NaF-AlF_3$ may also contain additives like CaF_2, MgF_2, and LiF. To understand the effect of added components on the structure and

* Author to whom correspondence should be addressed.
[†] Université de Liège.
[‡] Norwegian University of Science and Technology.
[⊗] Abstract published in *Advance ACS Abstracts,* June 1, 1996.

(1) Irish, D. E.; Ozeki, T. *Analytical Raman Spectroscopy, Chemical Analysis*; Wiley Interscience: New York, 1991; p 59.
(2) Dewing, E. W. *Metall. Trans.* **1989,** *20B*, 675.
(3) Gilbert, B.; Robert, E.; Tixhon, E.; Olsen, J. E.; Østvold, T. *Light Met.* **1995**, 181.
(4) Foster, P. A.; Frank, W. B. *J. Electrochem. Soc.* **1960,** *107*, 997.
(5) Dewing, E. W. *Metall. Trans.* **1990,** *21B*, 285.
(6) Sterten, Aa.; Mæland, I. *Acta Chem. Scand.* **1985,** *A39*, 241.
(7) Grjotheim, K.; Krohn, C.; Malinovský, M.; Matiasovskaý, K.; Thonstad, J. *Aluminium Electrolysis. Fundamentals of the Hall-Héroult Process*; Aluminium-Verlag: Düsseldorf, Germany, 1982; p 97.
(8) Rolin, M.; Bernard, M. *Bull. Soc. Chim. Fr.* **1962,** 429.
(9) Rolin, M.; Rey, M. *Bull Soc. Chim. Fr.* **1966**, 2785.
(10) Gilbert, B.; Begun, G. M.; Mamantov, G. *J. Chem. Phys.* **1975,** *62*, 950.
(11) Gilbert, B.; Materne, T. *Appl. Spectrosc.* **1990,** *44*, 299.
(12) Dewing, E. W. In *Proceedings of the Fifth International Symposium on Molten Salts;* Saboungi, M. L., Newman, D. S., Johnson, K., Inman, D., Eds.; The Electrochemical Society Proceedings 86; The Electrochemical Society: New York, 1986.
(13) Robert, E.; Materne, T.; Tixhon, E.; Gilbert, B. *Vib. Spectrosc.* **1993,** *6*, 71.
(14) Tixhon, E.; Robert, E.; Gilbert, B. *Appl. Spectrosc.* **1994,** *48*, 1477.

S0020-1669(95)01660-0 CCC: $12.00

on the technical important properties of cryolite-based melts, we decided to reinvestigate the $NaF-AlF_3$ system with additions of CaF_2 and MgF_2 in more detail. CaF_2 is the most commonly used additive in aluminium electrolysis. It is added in the bath as CaO, which is an impurity in the alumina. This calcium oxide reacts with the melt to form dissolved CaF_2 and Al−O−F complexes. Generally, its concentration is around 5 wt %. MgF_2 is sometimes added to the bath to improve some of its physicochemical properties. Moreover, Mg^{2+} and Ca^{2+} are both alkaline earth elements, and the comparison of their behavior is interesting from a fundamental point of view.

General background material for this work can be found in ref 7.

Experimental Section

Chemicals. Na_3AlF_6 was hand-picked cryolite from Greenland. The cryolite was dried under reduced pressure (10^{-4} atm) at 250 °C overnight.

MgF_2 and CaF_2, were "Zur Analyse", E. Merck. The salts were dried under reduced pressure (10^{-4} atm) at 200 °C for 10 h.

AlF_3, "Fiber grade", The British Drug House, was sublimated once for vapor pressure and two times for Raman studies.

All chemicals were handled in a glovebox with dry nitrogen containing less than 1 ppm of water vapor.

Vapor Pressure Measurements. Apparatus. The boiling point method described by Motzfeldt, Kvande, and Wahlbeck[15] was chosen for our measurements since this method gives reliable data in the pressure region 10^{-2} to 1 atm and at high temperatures (i.e., 1000−1300 °C). An apparatus specially designed for measurements of corrosive gases was readily available at the Institute of Inorganic Chemistry and has been described in detail by Herstad and Motzfeldt.[16] The main components of the equipment are a cold wall vacuum furnace with a vertically mounted graphite tube heater.

A cylindrical graphite cell (Graphite-I-Tite, Carborundum Co., USA) with a threaded lid was used as the sample container. The vapor outlet from the cell was a capillary opening drilled through the lid, 0.5 mm in diameter and 10 mm in length. The graphite cell contained an inner glassy carbon crucible. This inner crucible was used to reduce instabilities in the recorded weights. These instabilities may be due to wetting properties at the graphite−melt interface.

An electronic thermobalance, designed and built by SINTEF, The Foundation of Scientific and Industrial Research at the Norwegian University of Science and Technology, was used to measure the weight change of the graphite cell as a function of time. The output from the balance could be monitored on a chart recorder or a computer. The loading capacity of the balance was 160 g with a sensitivity better than ±0.2 mg.

The temperature of the furnace was read and controlled by a calibrated Pt/Pt 10% Rh thermocouple in conjunction with an Eurotherm controller. The hot junction of the thermocouple was located about 3 mm below the bottom of the cell.

To carry through the boiling point measurements by measuring weight losses at different inert gas pressures at constant temperature, the apparatus was equipped with both a Ruska Digital Direct Reading pressure gauge (Model DDR-6000) and a Druck digital manometer (0−1200 mbar) to control and measure the inert gas pressure fast and accurately (better than 1×10^{-4} atm).

Procedure. About 12 g of salt was used in each boiling point experiment. Sample and apparatus were degassed in vacuum (10^{-5}) atm at 200 °C overnight before measuring weight losses at different inert gas pressures at constant temperature. The rates of weight losses vs inert gas pressure data were used to calculate the vapor pressure using the nonlinear least-squared analysis computer program MODFIT.[17]

In some of the experiments, corrections of the measured vapor pressure had to be done due to changes of the composition during a run. The correction method applied by Knapstad, Linga, and Øye[18] was used with some modifications.

In the ternary systems $NaF-AlF_3-MgF_2$ and $NaF-AlF_3-CaF_2$, the main vapor species is still $NaAlF_4$.[19−21] The corrections made in the experimental vapor pressures were therefore performed as follows:

(i) The corrected vapor pressures for the binary system $NaF-AlF_3$ were plotted as a function of $x^\circ_{AlF_3}$ (where $x^\circ_{AlF_3} = n^\circ_{AlF_3}/(n^\circ_{AlF_3} + n^\circ_{NaF})$ and n°_i is the initial number of moles of component i) at 20 °C intervals in the measured temperature range.

(ii) The measured vapor pressures for the ternaries were fitted to the equation

$$\log(p_{tot}/\text{mbar}) = A - B/T$$

for each sample, assuming constant composition.

(iii) By comparing points i and ii at a given temperature, $x^\circ_{AlF_3}$ of the binary, which corresponded to the measured pressure could be obtained.

(iv) The slope of the vapor pressure vs $x^\circ_{AlF_3}$ at this binary concentration was used to perform the correction.

In the paper by Zhou *et al.*[22] the vapor pressures were corrected assuming that an increasing MgF_2 concentration during a measurement would dominate the change in pressure. This is, however, not the case since the evaporation of $NaAlF_4$ only gives minor changes in this concentration. The main change occurs in the cryolitic ratio, $CR = n_{NaF}/n_{AlF_3}$, (n = number of moles) due to evaporation of acidic species only. This must be reflected in the correction procedure.

Raman Spectroscopy. The spectra have been recorded using the same procedure and experimental set-up as reported earlier[11] except for some details that are reported below. All the chemicals were dried under vacuum at 400 °C overnight and the AlF_3 was further purified by two sublimations at 1000 °C under vacuum in a graphite container. To avoid problems due to oxide impurities, we found it necessary to prepare all our mixtures in a drybox in which the water content was below 2 ppm. For all the mixtures, the required amounts of solids were first crushed and mixed in an agate mortar. The solid powder was then premelted under argon atmosphere in a vitreous carbon crucible to ensure homogeneity. To record the spectra, an adjusted weight of the premelted mixture was introduced into a windowless graphite cell, which was contained in a quartz tube under argon atmosphere. The tube was then heated in a furnace specially designed for Raman measurements under constant temperature (±5 °C). The graphite cells were degassed one night under vacuum at 1000 °C before use. Our spectra are recorded using a Coherent Radiation Model 52-B argon-ion laser (300 mW, 488.0 nm) and a modified Cary 81 spectrometer interfaced with a microcomputer, allowing fast recording rates. Slit width of 5 cm^{-1}, a time constant of 0.1 s, and a scan rate of 250 cm^{-1} /min were used for each spectrum. In order to improve the signal over noise ratio, the spectra have been recorded several times and averaged. However, due to evaporation, the melt composition is likely to change with time. The averaging procedure is then applied only when no variation in the spectra is observed, otherwise only the first spectrum is used for further analysis. Finally, smoothing was never applied to the recorded spectra.

Results

Vapor Pressures. Total vapor pressures of liquid mixtures of $NaF-AlF_3$ were obtained with *CR* varying from 3 to 1 and with additions of MgF_2 and CaF_2. In Figures 1 and 2 $\log p_{tot}$ vs $1/T$ K^{-1} data are presented.

(15) Motzfeldt, K.; Kvande, H.; Wahlbeck, P. G. *Acta Chem. Scand.* **1977,** *A31,* 444.
(16) Herstad, O.; Motzfeldt, K. *Rev. Hautes Temp. Refract.* **1966,** *3*, 291.
(17) Hertzberg, T. Modfit - A general computer program for nonlinear parameter estimation. Institute of Chemical Engineering, University of Trondheim, NTH, Norway, 1983.
(18) Knapstad, B.; Linga, H.; Øye, H. A. *Ber. Bunsen-Ges Phys. Chem.* **1981,** *85*, 1132.
(19) Kvande, H. Thesis, Institute of Inorganic Chemistry, NTH, University of Trondheim, Norway, 1979.
(20) Guzman, J. Thesis, Institute of Inorganic Chemistry, NTH, University of Trondheim, Norway, 1986.
(21) Guzman, J.; Grjotheim, K.; Østvold, T. *Light Met.* **1986**, 425.
(22) Zhou, H.; Herstad, O.; Østvold, T. *Light Met.* **1991**, 511.

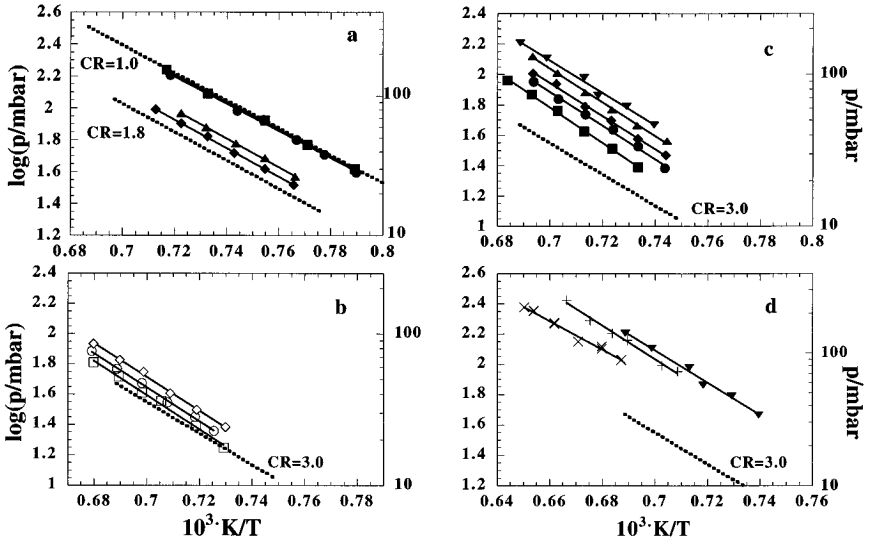

Figure 1. Vapor pressures at varying temperatures and *CR* for the system $NaF-AlF_3-MgF_2$. Data in part a are from the present work. Parts b−d show corrected data from Zhou *et al.*[22] Dotted lines are for the $NaF-AlF_3$ system. (a) Vapor pressures at varying temperatures and *CR* for the system $NaF-AlF_3-MgF_2$ at different $x°_{MgF_2}$: (■) $x°_{MgF_2} = 0.111$; (●) $x°_{MgF_2} = 0.250$; (◆) $x°_{MgF_2} = 0.0820$; (▲) $x°_{MgF_2} = 0.192$. (b) Vapor pressures at varying temperatures and $x°_{MgF_2}$ for the system $NaF-AlF_3-MgF_2$ at $CR = 3.0$: (□) $x°_{MgF_2} = 0.027$; (○) $x°_{MgF_2} = 0.0588$; (◇) $x°_{MgF_2} = 0.0968$. (c) (■) $x°_{MgF_2} = 0.143$; (●) $x°_{MgF_2} = 0.200$; (◆) $x°_{MgF_2} = 0.273$; (▲) $x°_{MgF_2} = 0.368$; (▼) $x°_{MgF_2} = 0.500$. (d) (▼) $x°_{MgF_2} = 0.500$; (+) $x°_{MgF_2} = 0.586$; (×) $x°_{MgF_2} = 0.692$.

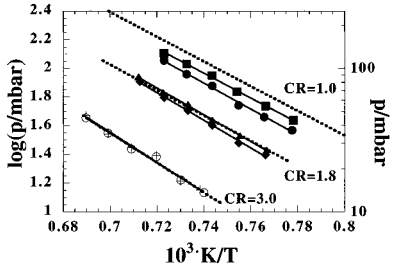

Figure 2. Vapor pressures at varying temperatures and $x°_{CaF_2}$ for the system $NaF-AlF_3-CaF_2$. (■) $x°_{CaF_2} = 0.111$; (●) $x°_{CaF_2} = 0.250$; (◆) $x°_{CaF_2} = 0.192$; (▲) $x°_{CaF_2} = 0.0820$, (○) $x°_{CaF_2} = 0.0588$; (×) $x°_{CaF_2} = 0.200$; (- - -) $NaF-AlF_3$.

Raman Spectroscopy. In order to study the ionic structure of the molten $NaF-AlF_3$ system, spectra have been recorded in a composition range from $CR = 5.6$ to $CR = 1.8$, with and without addition of MgF_2 and CaF_2. Since the intensities of the bands are strongly influenced by temperature variations, we have kept the recording temperature constant for each series of spectra.

Examples of spectra of $NaF-AlF_3$ mixtures are shown in Figure 3. A detailed interpretation of the assignments and intensity variations of the bands as a function of composition and temperature has already been published.[11] In summary, the main species existing in a 1:1 mixture is AlF_4^-, with the fundamental vibrational bands observed at 622 cm^{-1} (ν_1, strong and polarized), 760 cm^{-1}, (ν_3, weak and depolarized), and 320 and 215 cm^{-1} (ν_4 and ν_2, medium and depolarized). Only these bands, all due to the AlF_4^- tetrahedron, were observed at the 1:1 mixture at temperatures between the melting point of $NaAlF_4$ up to 1260 K. When the mole fraction of NaF is gradually increased, two new bands appear: one band, strong and polarized at 560 cm^{-1}, and another band, weak and depolarized around 345 cm^{-1}. If the amount of NaF is increased further, two additional bands appear, one as a shoulder at 510 cm^{-1} (strong, polarized) and the other around 320 cm^{-1} (weak and depolarized). The equilibrium between these three groups of bands is clearly influenced by temperature, as it is shown in Figure 4. A decrease of temperature produces a shift from the 622 cm^{-1} band toward the 560 and 510 cm^{-1} bands.

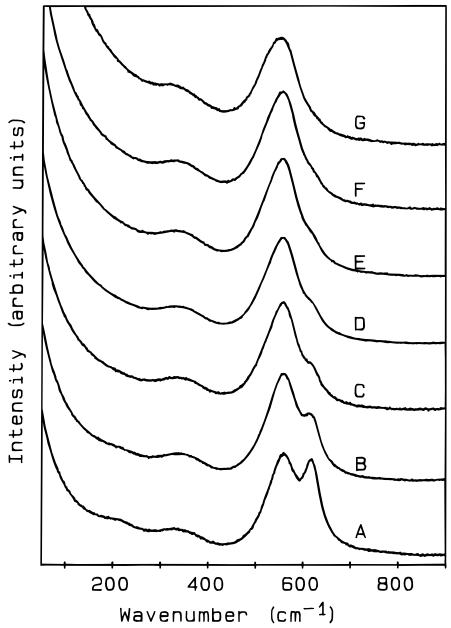

Figure 3. Spectra of molten $NaF-AlF_3$ mixtures at varying $x°_{AlF_3}$. $T = 1323$ K. Key: (A) 0.355; (B) 0.313; (C) 0.271; (D) 0.25; (E) 0.224; (F) 0.201; (G) 0.178; (H) 0.151.

Measurements of the Anion Distribution. Whatever the model is, the anion distribution can be calculated from the intensity of the bands and the determination of the scattering coefficient characteristic of each species (i.e., the proportionality coefficient which relates measured intensities with concentration).

(a) Determination of the Intensity Ratio of the Bands. Because of the difficulty involved in the precise reproduction of the molten drop shape and size in the windowless cell, only relative intensity measurements can be made. The general procedure for the extraction of the intensity ratio of the bands has been described in previous papers.[11,13] The various computer techniques used were very similar to the one described by Irish *et al.*[1] Briefly, the procedure consists of five steps: digital subtraction of the furnace blackbody emission if necessary (this emission background can be easily measured by

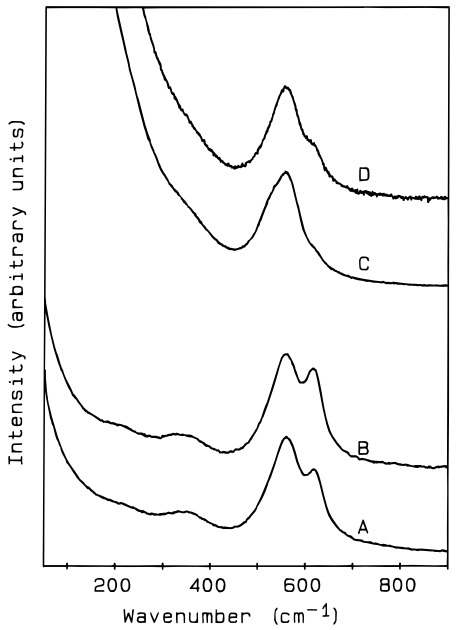

Figure 4. Spectra of molten NaF−AlF_3 (A and B) and NaF−NaCl−AlF_3 (C and D) mixtures at different temperatures: (A) $x°_{AlF_3} = 0.33$, $T = 1200$ K; (B) $x°_{AlF_3} = 0.33$, $T = 1293$ K; (C) $x°_{AlF_3} = 0.2$, $x°_{NaCl} = 0.2$, $T = 1123$ K; (D) $x°_{AlF_3} = 0.2$, $x°_{NaCl} = 0.2$, $T = 1293$ K.

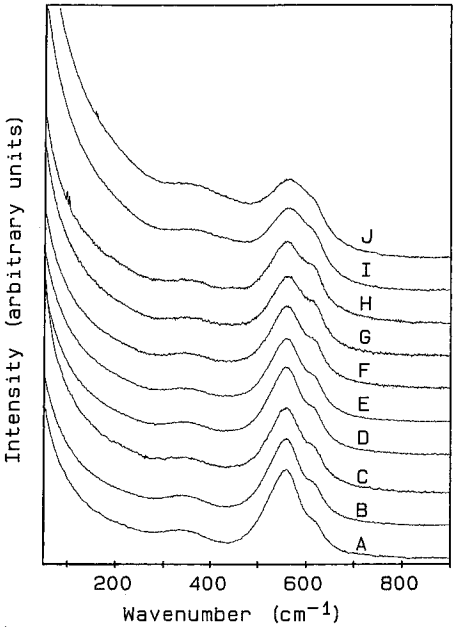

Figure 5. Spectra of molten NaF−AlF_3−MgF_2 mixtures with $CR = 2.61$ at varying $x°_{MgF_2}$. $T = 1293$ K. Key: (A) 0; (B) 0.03; (C) 0.071; (D) 0.08; (E) 0.099; (F) 0.122; (G) 0.179; (H) 0.2; (I) 0.296; (J) 0.4.

blocking the laser beam and recording the spectrum again); flattening of the Rayleigh light by an exponential quadratic function; subtraction of the 215 cm^{-1}, 320 cm^{-1} and 345 cm^{-1} bands by visual adjustment on the screen, if necessary; initial generation of a spectrum made of three components in order to obtain rough numbers for the height, width and position of the three remaining main bands; quantitative decomposition of the overlapping bands by a least square and simplex procedure. This procedure leads to the intensity ratios $I_{510}/I_{AlF_4^-}$ and $I_{560}/I_{AlF_4^-}$.

(b) Determination of the Scattering Coefficients. The scattering coefficients, D, have been measured from dilute solutions of NaF−AlF_3 in NaCl since these melts do not attack quartz. In addition, chlorofluoro species do not form, at least to a measurable extent. The spectra of nine NaF−AlF_3 mixtures

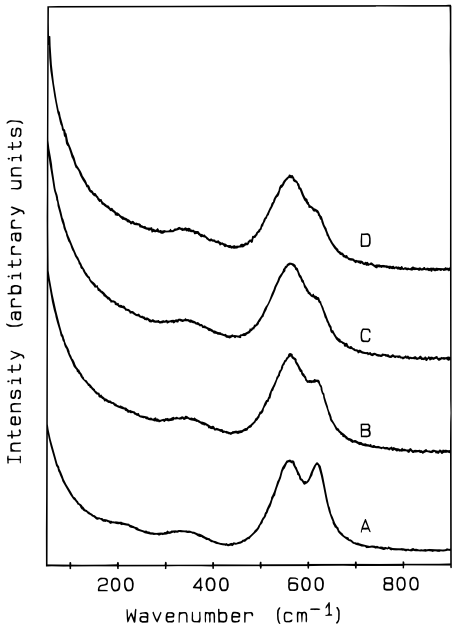

Figure 6. Spectra of molten NaF−AlF_3−CaF_2 mixtures with $CR = 1.78$ at varying $x°_{CaF_2}$. $T = 1273$ K. Key: (A) 0; (B) 0.098; (C) 0.149; (D) 0.2.

with $2 < CR < 4$ diluted in NaCl were recorded several times. These mixtures were contained in quartz tubings allowing a very good reproducibility of the absolute intensities. By keeping all the experimental conditions exactly constant, the intensities are directly comparable and no internal standard is necessary. To facilitate the calculations, the total amount of Al per unit volume was kept constant. The scattering coefficients were determined based on the surface area of a band and not the peak height. In addition, our procedure included a correction to take into account the narrowing of the bands on dilution. It is important to note that the results of these measurements do not depend on the exact nature of the species, but only on the number of Al per species. It is, however, reasonable to assume that the actual species contain only one Al per species. In this case, the resulting scattering coefficients, relative to AlF_4^- are as follows: $D_{510} = 2$; $D_{560} = 1.5$; $D_{AlF_4^-} = 1$.

(c) Determination of the Mole Ratios. Knowing the intensity ratio of the bands and their scattering coefficients, the mole ratio can be calculated. $n_{510}/n_{AlF_4^-} = (I_{510}/I_{AlF_4^-})/D_{510}$, and $n_{560}/n_{AlF_4^-} = (I_{560}/I_{AlF_4^-})/D_{560}$. Then, for 1 mol of mixture, assuming one aluminium per complex, we have that $n_{AlF_4^-} + n_{560} + n_{510} = n_{AlF_3}$. Using this equation and the two mole ratios, it is possible to calculate the number of moles of the three different species.

Examples of spectra of solutions of MgF_2 and CaF_2 in NaF−AlF_3 melts are presented in Figures 5 and 6. These data will be discussed below.

Discussion

The NaF−AlF_3 Binary System. Ionic Species. The model usually applied for ionic melts was first proposed by Temkin.[23] In this model anions and cations are distributed on anion and cation lattices, respectively. The present binary melt is traditionally considered to have one cation, Na^+ and several anions resulting from the dissociation of AlF_6^{3-}. We know with certainty from spectroscopy that one of these anions must be AlF_4^- (main band at 622 cm^{-1}). However, since the assignment

(23) Temkin, M. *Acta Physiochim.* **1945,** *20,* 411.

of the 510 and 560 cm^{-1} bands is still a subject of controversy,[24,25] we are going to examine the most probable hypotheses.

The Traditional Model (a). In the traditional model, the AlF_6^{3-} ion is assumed to dissociate into AlF_4^- and $2F^-$. From all our Raman data, this model must be rejected, since we clearly observe **three** sets of bands shifting in intensity with composition and temperature. We would like to point out that our previous spectroscopic work has not taken into consideration such a wide composition and temperature range as the one considered in this communication. Moreover, the quality of the present spectra is better, the resolution is higher, and no smoothing procedure has been applied. We may therefore state with confidence that all our results clearly indicate that there are two equilibria established in these melts.

Two Kinds of AlF_6^{3-} (b). It has been suggested by Brooker that the 560 cm^{-1} band could be due to isolated AlF_6^{3-} ions, and the shoulder at 510 cm^{-1} caused by an interaction between these ions and the Na^+ cations.[26] We have considered this model in more detail by calculating ionic concentrations based on our data. From the band intensities and the scattering coefficients, it is possible to determine the number of moles of AlF_4^-, AlF_6^{3-}, and $Na_xAlF_6^{x-3}$. From a simple mass balance, we can calculate the number of moles of free fluoride. Using Brooker's suggestion, for $x°_{AlF_3} > 0{,}27$, the fluoride concentration is **negative**. It is therefore evident that this model cannot match the whole composition range examined, and it must be rejected.

High Coordination Complex (c). We also considered the possibility that the 510 cm^{-1} band could be due to a higher coordinated complex, e.g., AlF_7^{4-}. Such a coordination around the small Al^{3+} ion has never been reported in the literature and is quite unlikely. Moreover, the coordination generally tends to decrease going from a solid to a liquid phase, and it is well-known that in the solid state Al^{3+} is six-coordinated.[27,28] Obviously, this model would also give negative concentrations of fluoride in the acidic range, and must be rejected.

AlF_5^{2-} Complex (d). In previous papers[11,13,14] the 560 cm^{-1} band was assigned to AlF_5^{2-} ions, and the 510 cm^{-1} band to AlF_6^{3-}. This model allows a consistent interpretation of the Raman data in the whole composition and temperature range. Moreover, when applied to the $KF-AlF_3$ binary,[14] good agreement with the results of Zhou,[29] who used vapor pressure measurements as a basis for a structural model of the binary, was observed. Dewing also proposed some reasonable arguments for the existence of the AlF_5^{2-} species.[12] Group theory, however, predicts two main bands for such a bipyramidal trigonal species, and only one band is observed. It is extensively discussed elsewhere,[14] that a phenomenon called pseudorotation may explain why only one band is observed at high temperatures. One way of assigning frequencies of species in the molten state is to compare the observed frequencies with frequencies from known species in the solid state. In the solid $NaF-AlF_3$ system, two different compounds exist; cryolite and chiolite.[27,28] The first one is made of isolated AlF_6^{3-} octahedrons and exhibits a main Raman band at 555 cm^{-1}.[24] The second is made of octahedrons sharing fluorides. The spectrum of solid chiolite has been recorded at room temperature, and its main band was found at 530 cm^{-1}. The AlF_6^{3-} ions in the molten phase are not supposed to share fluorides and we therefore observe an abnormal shift in frequency from 555 to 510 cm^{-1} for this species upon melting. This discrepancy is, however, mitigated by the fact that the main frequency of solid cryolite is lowered by about 15 cm^{-1} when the temperature is brought close to the melting point.[24] In addition, other examples of such shifts upon melting are known in the literature. For instance, Papatheodorou has shown that YCl_3-KCl mixtures contain the six-coordinated YCl_6^{3-} ion in both the solid and molten phase.[30] By increasing the temperature from 25 to 750 °C which is above the melting point, Papatheodorou found the ν_1 vibration shifted 24 cm^{-1}, 9%, toward a lower frequency. This shift was assigned to a weakening of the Y−Cl bond in the liquid. The shift we observe in the present study, from 555 to 510 cm^{-1}, is thus not incompatible with the assignment we propose. In any case, if the 555 cm^{-1} band was assigned to AlF_6^{3-}, the result would be the rejected model b with two kinds of AlF_6^{3-}.

$Al_2F_{10}^{4-}$ Complex (e). Another way to try to mediate for the problems introduced with the AlF_5^{2-} ion is to assume a melt consisting of AlF_4^-, AlF_6^{3-}, and a bridged, six-coordinated complex; $Al_2F_{10}^{4-}$. One can note that the stoichiometry of this complex is the same as for AlF_5^{2-}. To try to fit this model to our data, the scattering coefficients were recalculated to take into account a complex containing two Al. We have tested our data on the assignment

$$AlF_6^{3-},\ 510\ cm^{-1};\ Al_2F_{10}^{4-},\ 560\ cm^{-1};\ AlF_4^-,\ 622\ cm^{-1}$$

For this model we are facing the same problems with respect to pseudorotation and frequency change on melting which we met in case d. The pseudorotation process is much less favored with a bridged complex. In addition, thermodynamic data do not support the formation of $Al_2F_{10}^{4-}$.[12]

This model was therefore rejected.

Finally, we have to recall that the 510 cm^{-1} band we observe in the present melts is not due to an oxide contamination. We have shown a long time ago that oxide additions give rise to a band around 510 cm^{-1}. However, other bands are also appearing when oxide is added, such as the one at 200 cm^{-1}.[3] Since the 200 cm^{-1} band is absent in the present study and because of the behavior of the 510 cm^{-1} band as a function of, e.g., temperature, we can definitely rule out that the 510 cm^{-1} band is due to oxide in the melt.

Conclusion. We have seen that all the models in which the 560 cm^{-1} band is attributed to AlF_6^{3-} give negative fluoride concentrations in the acidic range. Despite of the shift in the AlF_6^{3-} frequency between solid and liquid, it seems as if the model based on AlF_4^-, AlF_5^{2-}, and AlF_6^{3-}, is the only one which can explain satisfactorily the Raman spectra in the whole composition range. In the present paper we will use this model in our further discussions.

Ionic Distribution. On the basis of the above discussion, we calculated from the spectra and the scattering coefficients the ionic concentrations of AlF_4^-, AlF_5^{2-}, AlF_6^{3-}, and F^-. These data are given in Figure 7. The main features of the plot representing the anion concentration vs $x°_{AlF_3}$ are as follows: the very low concentration of AlF_6^{3-} ions even at the cryolite composition; the maximum composition of AlF_6^{3-} does not seem to occur at the Na_3AlF_6 composition; the large concentration of AlF_5^{2-} at $x°_{AlF_3} > 0.15$. The measured concentration of AlF_6^{3-} is always very small. The AlF_6^{3-} band is present only as a shoulder, and during our band decomposition

(24) Brooker, M. H. *Proceedings from the H. A. Øye Symposium;* NTH: Trondheim, Norway, 1995, pp 431−434.
(25) Ratkje, S. K.; Cyvin, S. J.; Hafskjold, B. *Appl. Spectrosc.* **1993,** *47*, 375.
(26) Brooker, M. H. Private communication.
(27) Hawthorne, F. C.; Ferguson, R. B. *Can. Mineral.* **1975,** *13*, 377.
(28) Jacobini, C.; Leble, A.; Rousseau, J. J. *J. Solid State Chem.* **1981,** *36*, 297.
(29) Zhou, H. Thesis, Institute of Inorganic Chemistry, NTH, University of Trondheim, Norway, 1991.
(30) Papatheodorou, G. N. *J. Chem. Phys.* **1977,** *66*, 2893.

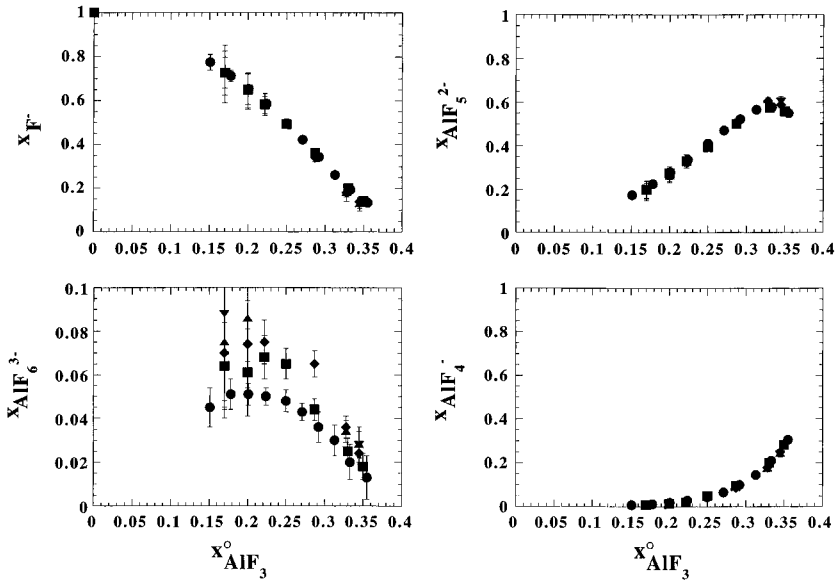

Figure 7. Ionic concentrations in $NaF-AlF_3$ melts as obtained from Raman spectra as a function of concentration and temperature: (●) 1323 K; (■) 1293 K; (◆) 1260 K; (▲) 1230 K; (▼) 1200 K. Bars indicate reproducibility of the Raman data.

procedure, the relative errors involved in its determination are large. This is why we do not consider the deviation of the expected location for the maximum content of AlF_6^{3-} as critical.

From the Raman data the stoichiometric equilibrium constants for the reactions

$$Na_3AlF_6(l) = Na_2AlF_5(l) + NaF(l) \quad (1)$$

$$Na_2AlF_5(l) = NaAlF_4(l) + NaF(l) \quad (2)$$

$$Na_3AlF_6(l) = NaAlF_4(l) + 2NaF(l) \quad (3)$$

can be calculated.

For eq 1 this constant is defined through the relation

$$K'_1 = \frac{a^{ideal}_{Na_2AlF_5} a^{ideal}_{NaF}}{a^{ideal}_{Na_3AlF_6}} \quad (4)$$

where the ideal activities are based on random mixing of the AlF_6^{3-}, AlF_5^{2-}, AlF_4^-, and F^- ions.

Using pure component standard states for the components of this ideal mixture, the activity of e.g., Na_3AlF_6 is unity at $CR = 3$. This can be obtained by defining

$$a^{ideal}_{Na_3AlF_6} = x_{AlF_6^{3-}}/x_{AlF_6^{3-}} \quad (CR = 3) \quad (5)$$

where $x_{AlF_6^{3-}}$ and $x_{AlF_6^{3-}}$ ($CR = 3$) are the real mole fractions of AlF_6^{3-} observed by Raman at a given CR and at $CR = 3$, respectively. At $CR = 3$ the weighed in mole fraction of AlF_3, $x^\circ_{AlF_3} = 0.25$. This implies that a_i^{ideal} for any component i formed in the melt at the stoichiometric composition of this compound is unity. When this definition is used, the data shown in Figure 8 are obtained. In this figure these constants are presented as ln K' vs $x^\circ_{AlF_3}$ plots for T/K = 1260, 1293, and 1323. For these temperatures only we have sufficient experimental data to make meaningful graphs. Straight line relationships are obtained within the uncertainty of the data except for a few experimental points. The main features of these graphs are the much larger value of K'_1 than K'_2 showing the stronger tendency of dissociation of the AlF_6^{3-} than of the AlF_5^{2-} ion,

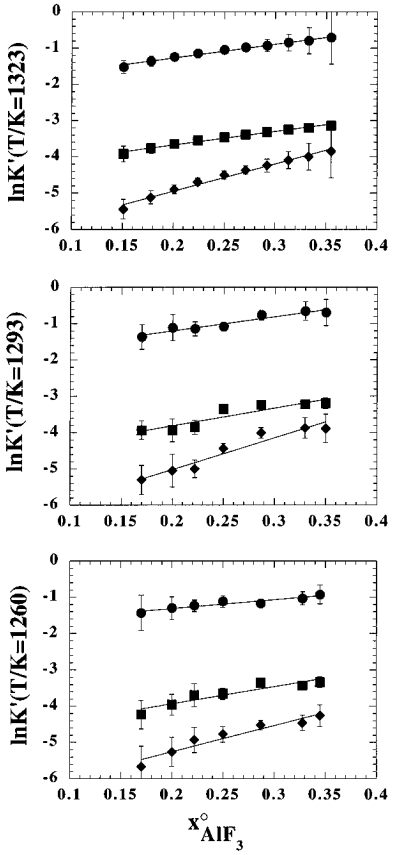

Figure 8. Stoichiometric equilibrium constants for reactions 1, 2, and 3 as functions of concentration at different temperatures: (●) K'_1; (■) K'_2; (◆) K'_3.

and the increasing tendency to dissociation of both AlF_6^{3-} and AlF_5^{2-} at higher AlF_3 concentrations. The temperature variations of the anion compositions at a given $x^\circ_{AlF_3}$ can also be calculated. In Figure 9 the stoichiometric equilibrium constants at $x^\circ_{AlF_3} = 0.17$, 0.25, and 0.35 are presented as ln K' vs $1/T$ (K^{-1}) plots for the temperature range investigated. Again straight line relationships are obtained within the uncertainty of the data. The variation of the slopes with composition may not be real, however, due to lack of precision in the concentration determinations of the anions. The negative slopes of these

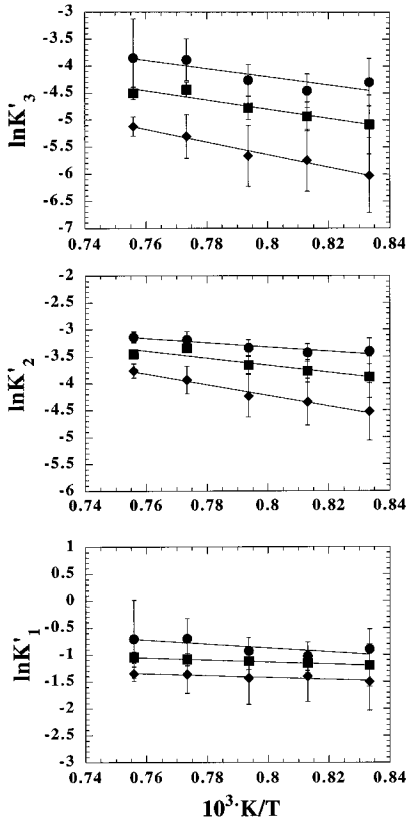

Figure 9. Stoichiometric equilibrium constants for reactions 1, 2, and 3 as functions of $1/T$ K^{-1} at three different mole fractions of AlF_3: (●) 0.35; (■) 0.25; (◆) 0.17.

lines, however, indicate positive reaction enthalpies. The magnitude of these reaction enthalpies has to be determined from activity data. This will be discussed below.

Activities. Dewing[5] and Sterten and Mæland[6] have probably presented the most reliable activity data for the binary liquid system $NaF-AlF_3$. When we compare the two data sets however, small differences are observed. The data of Dewing seem to be more accurate since somewhat irregular behavior is observed when the activity data presented by Sterten and Mæland are plotted vs concentration.[3] The activity data presented in this paper are therefore based on Dewing's paper. The activity data for NaF are given in Figure 10. On the basis of these data and the activity of AlF_3 as a function of composition, activities can be calculated for the $NaAlF_4$, Na_2AlF_5, and Na_3AlF_6 species. Using pure real liquid component standard states we obtain the results presented in Figure 10.

A small temperature variation in the activities may be observed. In Figure 11 the thermodynamic equilibrium constants for the reactions (1, 2, and 3) are given as ln K vs $1/T$ (K^{-1}) plots. The negative slopes observed show positive reaction enthalpies in agreement with the results shown in Figure 9.

The enthalpy, entropy and Gibbs energy changes for reactions (1, 2, and 3) are calculated on the basis of the above activity data and compared with other available thermodynamic data in Table 1. There is a fair agreement between the data of Dewing,[5] Sterten and Mæland[6] and Hong and Kleppa[31] for reaction 3 being the sum of reactions 1 and 2. This is also the only reaction from which data can be obtained from the JANAF tables.[31] When JANAF data are combined with the enthalpy of vaporisation for $NaAlF_4(l)$[19] an enthalpy change for reaction (3), ΔH_3° = 68 kJ, is obtained. This value is also in reasonable agreement with data given in Table 1 (71 kJ, 73 kJ). The reaction enthalpies calculated for reactions 1 and 2 from Dewing's activity data are in much better agreement with the calorimetric data of Hong and Kleppa than those calculated from the activity data of Sterten and Mæland. This difference may be due to the earlier mentioned irregularity in Sterten and Mæland's data.

From the above data, activity coefficients may be obtained for the species NaF, Na_3AlF_6, Na_2AlF_5 and $NaAlF_4$ for $x^\circ_{AlF_3} < 0.5$ using pure component standard states. The activity coefficients we want to present take into consideration the deviation from random distribution of the anions F^-, AlF_6^{3-}, AlF_5^{2-} and AlF_4^-, which we believe are present in the melt. For an ideal mixing of these ions all the activity coefficients

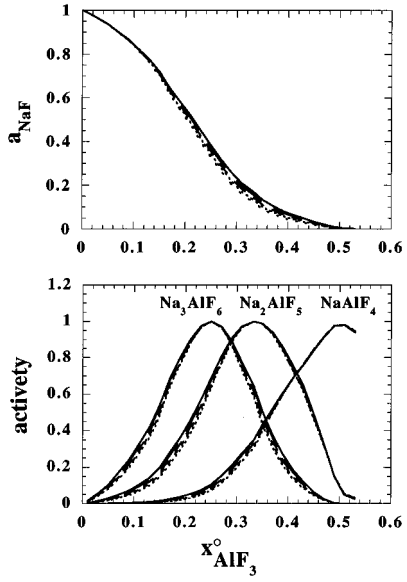

Figure 10. Activities calculated from data by Dewing[5] in the $NaF-AlF_3$ binary. Pure real liquid standard states were used in the calculation. Key: (—) 1323 K; (— —) 1293 K; (– –) 1260 K; (- - -) 1230 K; (···) 1200 K.

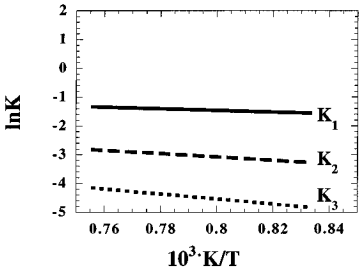

Figure 11. Thermodynamic equilibrium constants for reactions 1, 2, and 3 as a function of $1/T$ K^{-1}. Data from Dewing.[5]

Table 1. Thermodynamic Data for Reactions 1, 2, and 3 As Derived from the Data of Dewing,[5] Sterten and Mæland,[6] and Hong and Kleppa[31]

reaction	T/K	$\Delta H°$/kJ	$\Delta S°$/J	$\Delta G°$/kJ at 1293 K	ref
1	1298	24.6			31
		32.5	14.5	13.8	6
		24.6	7.5	15.0	5
2	1298	48.4			31
		38.5	4.9	32.3	6
		48.2	12.9	31.3	5
3	1298	73.0			31
		71.0	19.4	46.0	6
		72.8	20.4	46.4	5

(31) Hong, K. C.; Kleppa, O. J. *J. Phys. Chem.* **1978,** *82,* 176.

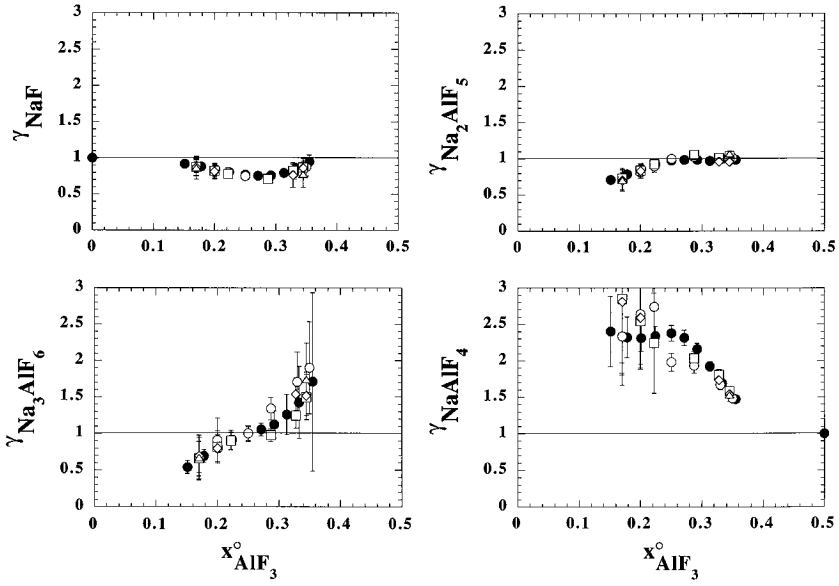

Figure 12. Raoultian activity coefficients of species observed by Raman in the $NaF-AlF_3$ binary. These coefficients were obtained using the data shown in Figures 7 and 10. Key: (●) 1323 K; (○) 1293 K; (□) 1260 K; (◇) 1230 K; (△) 1200 K.

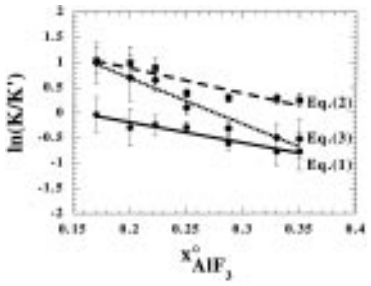

Figure 13. Ratios of the thermodynamic and stoichiometric equilibrium constants for reactions 1, 2, and 3 as functions of $x^\circ_{AlF_3}$ at 1293 K; calculated from a combination of the present results and the data of Dewing:[5] (●) eq 1; (■) eq 2; (◆) eq 3. Regression lines: (—) eq 1; (– –) eq 2; (- - -) eq 3.

will thus be unity. The real activity of e.g. Na_3AlF_6 is then

$$a_{Na_3AlF_6} = x_{AlF_6^{3-}}\gamma_{Na_3AlF_6}/x_{AlF_6^{3-}} \quad (CR = 3) \qquad (6)$$

and similarly for the other compounds shown to be present in this melt by Raman spectroscopy. The result of using eq 6 and similar equations for the other compounds are presented in Figure 12. The most important features of these plots are as follows.

$\gamma_i = 1$ for pure i according to the standard state chosen.

The deviation from 1 in these activity coefficients indicates that there is some deviation from random mixing of the anions of this binary melt mixture.

The largest absolute change in the activity coefficients vs composition is observed for $NaAlF_4$. γ_{NaAlF_4} varies from 3 to 1.5 in the concentration region $0.17 \le x^\circ_{AlF_3} \le 0.35$ depending somewhat on temperature.

Even though the activity coefficients are determined with some inaccuracy, it may be of interest to evaluate the contribution these activity coefficients have on the equilibrium constants of reactions 1–3. In Figure 13 ln K/K' is plotted vs $x^\circ_{AlF_3}$ at 1293 K using the data in Table 2. The most important features of these plots are as follows.

ln K/K' varies in the range −1 to +1 indicating a considerable difference between the thermodynamic and stoichiometric equilibrium constants for reactions 1–3.

The contribution to ΔG° for each reaction at $x^\circ_{AlF_3} = 0.25$ and $T/K = 1293$ from the activity coefficients, varies between −3.3 kJ for reaction 1 (ΔG°_1 (Dewing[5]) = 15 kJ) to 4.7 kJ for reaction 2 (ΔG°_2 (Dewing[5]) = 31.3 kJ).

The Ternary $NaF-AlF_3-MX$ (MX = MgF_2, CaF_2) Systems. Our comparison of the Raman and vapor pressure data will be based on the activity and concentration of $NaAlF_4$. This activity is the product of the concentration of $NaAlF_4$, $x_{AlF_4^-}$, and its activity coefficient since $x_{AlF_4^-}$ ($CR = 1$) = 1. The molar fraction $x_{AlF_4^-}$, is defined as $n_{AlF_4^-}/n^\circ$, where $n_{AlF_4^-}$ is the number of moles of AlF_4^-, directly calculated from the spectra, and n° is the total number of mole of anions. In the two ternaries $NaF-AlF_3-CaF_2$ and $NaF-AlF_3-MgF_2$, the calculation of $x_{AlF_4^-}$ is not straightforward, however, and will depend on a model chosen for the melt. The number of moles of AlF_4^-, AlF_5^{2-}, and AlF_6^{3-} are measured directly from the Raman spectra, but association between ions may occur in the melt and the total number of moles of anions will therefore depend on the degree of association. Since this association not necessarily will result in new bands in the spectra, n° may be difficult to calculate from the Raman spectra alone, and additional data are necessary to establish a proper basis for a model of the melt. This is why thermodynamic data in combination with Raman spectra give us a method to check if the model we use to explain the effect of an additive on the melt structure, is reasonable.

Acid–Base Properties. General Concepts. Before we compare Raman and vapor pressure data it may be useful to discuss the acid–base behavior of additives such as CaF_2 and MgF_2 since it is sometimes very easy to misinterpret if the additive is basic or acidic. From Figure 6, e.g., it is clearly seen that CaF_2 reduces the intensity of the AlF_4^- band relative to the two other bands. This observation may at first sight lead to the conclusion that CaF_2, when dissolved in the melt, releases F^- ions and in this sense behaves as a base. The action of CaF_2 is, however, more complex because one has to include the effect of dilution and association.

When a third component, MX, is added to a binary $NaF-AlF_3$ melt, the activities of NaF and AlF_3 will change. In a paper by Dewing[2] this problem has been discussed in detail. Dewing used the Gibbs–Duhem equation to show that the variation in a_{NaF} and a_{AlF3} with x_{MX} is given by

$$x_{NaF}\frac{d(\ln a_{NaF})}{dx_{MX}} + x_{AlF_3}\frac{d(\ln a_{AlF_3})}{dx_{MX}} = -1 \qquad (7)$$

Table 2. Equilibrium Constants and Stoichiometric Equilibrium Constants of Reactions 1, 2, and 3 at 1293 K

reaction	ln K (K) Sterten and Mæland[6]	ln K (K) Dewing[5]	ln K'	ln K' (K') ($x^\circ_{AlF_3} = 0.25$) present results
1	−1.280 (0.278)	−1.398 (0.247)	$-1.9717 + 3.854\, x^\circ_{AlF_3}$	−1.008 (0.365)
2	−2.996 (0.050)	−2.919 (0.054)	$-4.7897 + 4.875\, x^\circ_{AlF_3}$	−3.571 (0.028)
3	−4.276 (0.0139)	−4.317 (0.0133)	$-6.7615 + 8.729\, x^\circ_{AlF_3}$	−4.579 (0.010)

if the third component, *MX*, is diluted. Let us assume that the additive is neutral and that the activity coefficients of NaF and AlF_3 do not change. In this case

$$\frac{d(\ln a_{NaF})}{dx_{MX}} = \frac{1}{x_{NaF}} \times \frac{dx_{NaF}}{dx_{MX}}$$

For constant *CR*, $dx_{NaF}/dx_{AlF_3} = x_{NaF}/x_{AlF_3}$. Using this relation in combination with eq 7 we obtain

$$\frac{d(\ln a_{NaF})}{dx_{MX}} = \frac{d(\ln a_{AlF_3})}{dx_{MX}} \tag{8}$$

Combining this equation with eq 7 we get

$$\frac{d(\ln a_{NaF})}{dx_{MX}} = \frac{d(\ln a_{AlF_3})}{dx_{MX}} = -1 \tag{9}$$

for small values of x_{MX}.

Equations 8 and 9 define simple dilution by a neutral additive. Consequently, we can define an acidic or basic addition by $d(\ln a_{AlF_3}/dx_{MX} > -1$ or < -1, respectively.

Experimental Evaluation of Acid−Base Behavior. Both vapor pressure and Raman spectra give us information on the acidity of an additive. The vapor over $NaF-AlF_3$ melts is predominantly $NaAlF_4$ formed by the reaction

$$NaF + AlF_3 = NaAlF_4 \tag{10}$$

having an equilibrium constant K_{10}. This gives

$$a_{NaAlF_4} = p_{NaAlF_4}/p^\circ_{NaAlF_4} = K_{10} a_{NaF} a_{AlF_3} \tag{11}$$

and in combination with eq 7 we obtain according to Dewing[2]

$$\frac{d(\ln a_{AlF_3})}{dx_{MX}} = \frac{CR}{CR-1}\left(\frac{d\ln(p_{NaAlF_4}/p^\circ_{NaAlF_4})}{dx_{MX}} + \frac{CR+1}{CR(1-\bar{x}_{MX})}\right) \tag{12}$$

where $p^\circ_{NaAlF_4}$ is the pressure of $NaAlF_4$ above pure $NaAlF_4$, and $\bar{x}_{MX}$ is the value of x_{MX} at the center of the range of x_{MX} used.

When $CR \rightarrow 1$, eq 12 is not easy to use since the first term approaches infinity and the term in the paranthesis approaches zero. Using a combination of eqs 7 and 11 for $CR = 1$ and eqs 9 and 11 for any *CR* gives

$$d(\ln a_{NaAlF_4})/dx_{MX} = [d(\ln p_{NaAlF_4})/p^\circ_{NaAlF_4}]/dx_{MX} = -2 \tag{13}$$

for $CR = 1$ or for any *CR* when the additive is neutral. Equation 13 shows that the bracketed part in eq 12 approaches zero when $CR = 1$ as mentioned above.

The experimental measurement of the pressures and its variation upon addition of a third component allows us to estimate the acidity of the additive through eq 12. In these calculations we may use the data of Kvande[19] to obtain $p^\circ_{NaAlF_4}$. Kvande gives

$$\ln p^\circ_{NaAlF_4}/\text{atm} = 5.301 - 8573/T\,\text{K}^{-1} \tag{14}$$

This equation gives $p^\circ_{NaAlF_4} = 47.5$ mbar at 1293 K in agreement with the calculated pressure, 49 mbar, obtained by Dewing.[5] To obtain partial pressures of $NaAlF_4$ from total pressures some corrections must be made. In both ternary systems the presence of Mg or Ca containing vapor species is neglected. This assumption is based on mass spectrometric data from Guzman.[20] Both Guzman[20] and Zhou *et al.*[22] showed that the main vapor species above the present melts will be $NaAlF_4$, $Na_2Al_2F_8$, and NaF. The dimer pressure is obtained using the reaction

$$2NaAlF_4(g) = Na_2Al_2F_8(g) \tag{15}$$

The equilibrium constant, K_{15}, is given by Kvande.[19] The partial pressure of NaF is obtained using activity data from Dewing[5] and p°_{NaF} data are given in JANAF.[32] The partial pressure of $NaAlF_4$ is then obtained from the equation

$$K_{15} p^2_{NaAlF_4} + p_{NaAlF_4} + p_{NaF} - p_{tot} = 0 \tag{16}$$

and the acidity of the additive may then be evaluated using eq 12.

If the additive is basic a_{NaAlF_4} or the $NaAlF_4$ pressure will decrease more per *MX* added than given by eq 13. If this decrease is given by a number *k*, eq 13 may be integrated, and the resulting ternary activity coefficient of $NaAlF_4$ can be calculated by the equation

$$\gamma_{NaAlF_4}(t) = \gamma_{NaAlF_4}(b)\frac{x_{AlF_4^-}(b)}{x_{AlF_4^-}(t)}\exp(-kx_{MX}) \tag{17}$$

where t stands for the ternary and b for the binary melts, respectively. Equation 17 can be used to show how the activity coefficients of $NaAlF_4$ will vary when *MX* is added in small amounts to the $NaF-AlF_3$ binary. This procedure to obtain ternary activity coefficients will be compared with a method to obtain variations in γ_{NaAlF_4} from Raman data only. The latter method is based on a fitting procedure using a computer model. This model is able to reproduce an experimental Raman spectrum of any $NaF-AlF_3$ binary melt having $5 > CR > 1$. A binary model melt having the same intensity profiles for the AlF_4^-, AlF_5^{2-}, and AlF_6^{3-} Raman bands as in the ternary is selected. The unknown activity coefficient of e.g., $NaAlF_4$ in the ternary is approximated by the activity coefficient of $NaAlF_4$ in this binary. This coefficient may be estimated for any additive introduced to the $NaF-AlF_3$ binary.

We have found that small additions of a third component, *MX*, will change significantly the distribution of the AlF_4^-, AlF_5^{2-}, and AlF_6^{3-} ions. This may in our opinion indicate changes in the activity coefficients of the $NaAlF_4$, Na_2AlF_5, and Na_3AlF_6 compounds, since these activity coefficients vary with *CR* as observed from our Raman data on the binary. In Table 3 activity coefficients of $NaAlF_4$ calculated by eq 17 are compared with those obtained from $NaF-AlF_3$ binaries giving the same Raman spectra as the ternary. Very good agreement

(32) *JANAF Thermochemical Tables* **1985**, *14*.

Table 3. Activity Coefficients of $NaAlF_4$ in Ternary $NaF-AlF_3-MX$ Melts Calculated as a Function of *MX* Additions at Different *CR* Using Eq 17 and Raman Data Only

$$x^\circ_{MX} = n^\circ_{MX}/(n^\circ_{MX} + n^\circ_{NaF} + n^\circ_{AlF_3})$$

		γ_{NaAlF_4}	
system	x°_{MX}	Raman	eq 17
CaF_2, $CR = 3$	0	2.8	2.8
T/K = 1293	0.049	2.9	3.4
	0.0961	3.0	3.5
	0.1506	3.1	3.5
	0.204	3.3	3.6
	0.2563	3.4	3.7
	0.299	3.5	3.8
CaF_2, $CR = 1.8$	0	1.5	1.5
T/K = 1273	0.098	1.8	1.8
	0.149	2.0	2.1
	0.206	2.2	2.1
MgF_2, $CR = 3$	0	2.5	2.5
T/K = 1293	0.0395	2.3	2.1
	0.0617	2.2	2.0
	0.0796	2.2	1.9
	0.0986	2.2	1.8
MgF_2, $CR = 2.15$	0	2	2
T/K = 1293	0.0282	1.9	1.6
	0.0613	1.7	1.6
	0.0781	1.6	1.5
	0.1022	1.6	1.5
	0.1300	1.5	1.4

is observed. This indicates that the procedure developed to obtain activity coefficients in ternary melts from Raman data only, may be used to calculate thermodynamic data for ternary mixtures.

The vapor pressures above cryolitic melts can then be calculated using the equation

$$p_{NaAlF_4} = p^\circ_{NaAlF_4} a_{NaAlF_4} = p^\circ_{NaAlF_4} x_{Na^+} x_{AlF_4^-} \gamma_{NaAlF_4} \qquad (18)$$

where γ_{NaAlF_4} is the Raman based activity coefficient of $NaAlF_4$.

The activity coefficients we have used for the $NaF-AlF_3$ binary to calculate vapor pressures above the ternary melts are those given in Figure 14. These coefficients have been obtained by combining Raman and vapor pressure data for this binary, and they therefore deviate somewhat from those obtained using our Raman data and activities from Dewing.[5] The difference is, however, within experimental error.

A comparison of the measured vapor pressures with those calculated from Raman data are presented below. CaF_2 and MgF_2, respectively, are added to the $NaF-AlF_3$ binary for varying *CR*. The acid−base properties of CaF_2 and MgF_2 are also discussed.

MgF_2 Additions. For the system $Na_3AlF_6-MgF_2$ data have been presented by Guzman *et al.*,[21] Zhou *et al.*,[22] and Dewing.[33] The first two papers give vapor pressures while Dewing presents activity data of Na and Mg in liquid Al in equilibrium with $NaF-AlF_3-MgF_2$ melts. Due to changes in melt composition with time during vapor pressure measurements with the boiling point method, it is necessary to perform corrections of such data to obtain the pressure at correct composition. In the work by Zhou *et al.*,[22] as mentioned earlier, this correction was performed erroneously. Guzman did not correct his raw data. A proper correction of Zhou's data was performed by us and our results are then compared with the data of Dewing.[33] Results are given in Figure 15 and show good agreement for

(33) Dewing, E. W.; van der Kouwe, E. Th. *Light Met.* **1989**, 297.

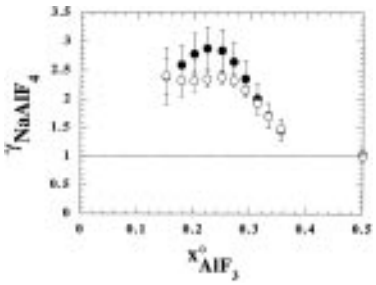

Figure 14. Activity coefficients of $NaAlF_4$ in the $NaF-AlF_3$ binary. $T = 1323$ K. Key: (●) present work; (○) present Raman data combined with activity data from Dewing.[5]

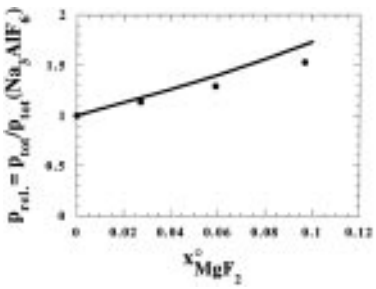

Figure 15. The relative pressure as a function of $x^\circ_{MgF_2}$ given as the measured pressure for the $NaF-AlF_3-MgF_2$ ternary divided by the pressure of the $NaF-AlF_3$ binary at $CR = 3$. Key: (●) corrected data from Zhou *et al.*;[22] (−) data from Dewing.[33]

small MgF_2 additions. Small deviations occur for $x_{MgF_2} > 0.04$, but considering the experimental error, the agreement is good over the whole concentration range.

The vapor pressure data presented in Figure 1 show increasing vapor pressures with MgF_2 additions as long as $CR > 1$. At $CR = 1$ the vapor pressure remains almost constant, as can be observed from Figure 1 where $\ln p_{tot}$/mbar is plotted vs $x^\circ_{MgF_2}$ at $CR = 1$, although the dilution effect of adding MgF_2 to $NaAlF_4$ should have decreased the pressure. A simple explanation could be that MgF_2 is not very soluble in pure $NaAlF_4$. Indeed, Raman spectra of $NaAlF_4-MgF_2$ mixtures have been recorded showing spectra identical to the pure $NaAlF_4$ spectrum. Solid particles could also be observed in the molten drop, indicating a low MgF_2 solubility. The observation of constant vapor pressure may also imply that in this very acidic melt, where a_{AlF_3} is increased by a factor of ≈ 1000 relative to a_{AlF_3} in Na_3AlF_6, new vapor species may be formed. A possible reaction may be

$$MgF_2(l) + AlF_3(l) = MgAlF_5(g) \qquad (19)$$

At $CR = 1.8$, a_{AlF_3} is increased by a factor of only 10 relative to data at $CR = 3$, and the formation of Mg containing complexes is probably much less likely to occur. It is indeed verified at $CR = 3$ by mass spectrometric data[20] that Mg-containing species form to a much smaller extent than NaF- and AlF_3-containing gas complexes.

Our data show that MgF_2 is an acidic additive and will tend to form MgF_3^- or MgF_4^{2-} species. This has also been proposed by Zhou *et al.*[22] and Dewing,[33] and their results are in qualitative agreement with our data. This can also be observed from data presented in Table 4 where eqs 7, 12, and 16 have been used to obtain the acid character of MgF_2 in these melts.

In order to identify species formed when MgF_2 is added to cryolitic melts, spectra of $NaF-MgF_2$ melts were first recorded. The shape of the spectra, the number of bands and their polarization correspond to a tetrahedral species, MgF_4^{2-}, whose main ν_1 mode occurs at 430 cm^{-1}. For additions of MgF_2 higher

Table 4. Activity Change of NaF and AlF_3 and the Change in Pressure of $NaAlF_4$ on Addition of a Third Component, *MX*, Where $\bar{x}_{MX}$ Is the Average Value of the $x°_{MX}$ Values Used

additive, *MX*	*CR*	$\bar{x}_{MX}$	$d(\ln(p/p°))/dx_{MX}$,[b] eq 16	$d(\ln a_{AlF_3})/dx_{MX}$, eq 12	$d(\ln a_{NaF})/dx_{MX}$, eqs 7 and 12
CaF_2	3	0.1	0 ± 1.7	2.0 ± 2.5	-2.0 ± 0.8
	1.8	0.1	-0.9 ± 0.6	1.9 ± 1.3	-2.8 ± 0.7
	1	0.12	-1.6 ± 0.3	*a*	*a*
MgF_2	3	0.1	3.9 ± 1.6	8.1 ± 2.4	-4.2 ± 0.8
	1.8	0.1	1.6 ± 0.4	7.5 ± 0.9	-5.9 ± 0.5
	1	0.12	-0.2	*a*	*a*
MX, acid or base	1		-2		
neutral	*CR*		-2	-1	-1

[a] Not defined. [b] The numbers in this column are obtained from eq 16 and are equal to $-k$ in eq 17.

than 25 mol %, two bands are growing on the sides of the ν_1 of MgF_4^{2-}, at about 470 and 375 cm^{-1}. These bands could be the sign of the formation of some bridged complex, such as $Mg_2F_6^{2-}$.

As can be seen from Figure 5, the addition of MgF_2 to NaF−AlF_3 produces two immediately visible modifications of the spectra: a change in the intensity ratios of the three ν_1 bands of the Al−F complexes, corresponding to a displacement from AlF_6^{3-} toward AlF_5^{2-} and AlF_4^-; a band at 430 cm^{-1} becoming visible with a half-height band width of 110 cm^{-1} and overlaping with the ν_1 band of AlF_6^{3-} and with the Al−F bands at 350 cm^{-1}. This band indicates that Mg certainly keeps its tetrahedral coordination in these ternary melts. Furthermore, a close analysis shows that the profile of the 430 cm^{-1} band is modified when the amount of MgF_2 increases. It seems also as if the two bands observed in the NaF−MgF_2 binary are present in the ternary for high MgF_2 contents (>15 mol %). However, if a bridged complex, such as $Mg_2F_6^{2-}$ is formed, it is always a minor species compared to the tetrahedral complex.

Finally, it was found that the ν_1 band of AlF_5^{2-} is strongly influenced by the addition of magnesium fluoride. Not only its band width, but also its position is largely affected. In cryolite the addition of 40 mol % of MgF_2 produces a broadening as large as 20%, from 82 to 98 cm^{-1}, and an increase of the frequency from 560 to 572 cm^{-1}. The broadening and the displacement of the band frequency are directly proportional to the amount of MgF_2 for a given *CR*. In addition, the overall effect is even stronger when the *CR* decreases, i.e., when the medium is less basic. This behavior indicates a special kind of interaction between MgF_2 and AlF_5^{2-}.

If MgF_2 dissolves by forming MgF_4^{2-} ions, there are not always enough free fluorides to satisfy the tetrahedral coordination of the magnesium. Consequently, one part of the magnesium fluoride is then necessarily strongly solvated by some Al−F species, since a bridged $Mg_2F_6^{2-}$ complex is always a minor species compared with the tetrahedral one. Moreover, if the dimer was formed to a large extent, the deformation of the solvent bands would not be observed.

If we consider that AlF_5^{2-} is the main solvating species, the experimental observations may be explained. If the AlF_5^{2-} anion shares one of its fluorides with the magnesium, this Al−F bond will be weakened and, as a consequence, the four other Al−F bonds will be reinforced, moving the frequency of their vibration to higher values. This interaction also involves a broader distribution of the frequencies, resulting in a broadening of the band. In addition, the tendency to share a fluoride with the solvent will be larger when less free fluorides are available, i.e., in less basic melts, as observed. It is interesting to note that, even in acidic melts, the AlF_4^- band is not strongly affected by MgF_2 addition. A shift of frequency is never observed, and a small broadening occurs in acidic melts only, for very high concentrations of MgF_2 (>30 mol %). This indicates a more rigid complex which does not easily share its fluorides.

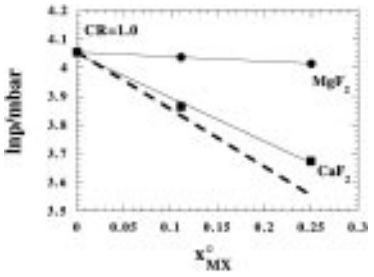

Figure 16. ln (p_{tot}/mbar) as function of $x°_{MX}$, at $CR = 1$ for MgF_2 and CaF_2 additions. $T = 1293$ K. Dotted line: Theoretical.

In order to quantify the acidity variation occurring on MgF_2 additions, we have limited our analyses to the spectra for which the variation of band width and frequency is small, i.e., for mixtures with low MgF_2 contents (up to 10−15 mol % depending on the acidity of the solvent). As we only consider spectra for which the profile and the position of the bands are not much modified, we will use the scattering coefficients and equilibrium constants of the pure solvent. Furthermore, because of the low Mg concentration, we will neglect the formation of bridged Mg species in our calculations.

The distributions of the various Al−F species have been measured in the system NaF−AlF_3−MgF_2, where $CR = 2.15$, 2.61, and 3. From each mixture, the band of the Mg complex must be subtracted from the spectra, since it overlaps with the AlF_6^{3-} band. The same procedure as for the subtraction of the 215, 320, and 345 cm^{-1} bands of the solvent was used. Therefore, as shown above, we can calculate the number of moles of AlF_4^-, AlF_5^{2-} and AlF_6^{3-}. Then, using the fluoride mass balance and the equilibrium constants of eqs 1 and 2 of the solvent, the number of moles of free F^- has been calculated assuming the reaction scheme below, where magnesium is always kept four-coordinated.

$$MgF_2 + nF^- + (2-n)AlF_5^{2-} \rightarrow MgF_{2+n}(AlF_5)_{2-n}^{(4-n)-} \quad (20)$$

Here *n* varies from 0 to 2. Knowing the initial compositions the amount of MgF_2 added and the final F^- content, it is possible to calculate the average number of moles of F^-, $\bar{n}_F$, which has been consumed for each mole of MgF_2 added. For a constant *CR*, $\bar{n}_F$ decreases when the amount of magnesium fluoride increases. On the other hand, the magnitude of $\bar{n}_F$ increases with the *CR*. If the solvent is more basic, there are more free fluorides in the medium, and MgF_2 can consume more F^-. On the contrary, if the solvent is more acidic there are fewer fluorides available and $\bar{n}_F$ is thus lower.

Having the ionic composition from the model calculations, the vapor pressures are calculated using eq 18. We obtain the data shown in Figure 17. The calculated pressures are in reasonable agreement with measured values up to $x_{MgF_2} = 0.1$. From the distribution of the three fluoroaluminate species in acidic melts calculated from the Raman spectra, we know that

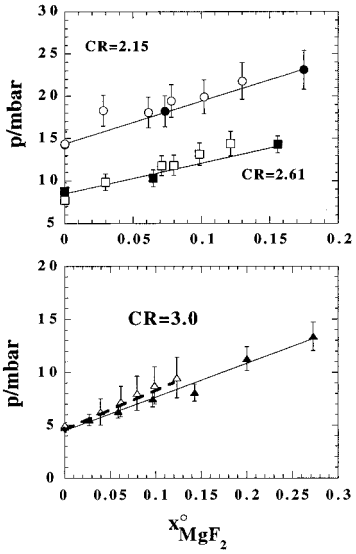

Figure 17. Experimental and calculated vapor pressures above NaF−AlF_3−MgF_2 melts at 1293 K. The experimental pressures at $CR = 2.15$ and 2.61 are interpolated data. $CR = 2.15$: (●) observed; (○) calculated. $CR = 2.61$: (■) observed; (□) calculated. $CR = 3$: (▲) observed; (△) calculated; (− −) based on MgF_4^{2-} and $Mg_2F_6^{2-}$ as suggested by Dewing.[33]

very little MgF_4^{2-} can be formed, since the formation of mainly MgF_4^{2-} would probably lead to a larger shift of the equilibria toward AlF_4^- than observed. The bridged complexes suggested between Mg^{2+} and AlF_5^{2-} explain the observed change in pressures. This supports our model.

On the basis of MgF_2 activity data measured for MgF_2−Na_3AlF_6 mixtures, however, Dewing[33] suggested the formation of the MgF_4^{2-} and $Mg_2F_6^{2-}$ anions. His model also fits very well with the measured pressures as can be observed in Figure 17 for $CR = 3$.

CaF_2 Additions. When CaF_2 is added to the NaF−AlF_3 binary, only minor vapor pressure changes are observed in the concentration range $2 < CR < 3$, as can be seen from Figure 2. In more acidic melts a lowering of the pressure occurs. However, this decrease does not necessarily indicate a basic behavior, as we previously thought. Dewing[2] showed that a neutral diluent should decrease the vapor pressure according to eq 13. At $CR = 1$ the decrease observed in Figure 16 is in agreement with eq 13.

The decrease observed by CaF_2 additions for $CR = 3$ and 1.8 as can be observed from Table 4, indicate a weak acidic behavior. Such a result seems, at first sight, to be contradictory to the Raman data. Addition of CaF_2 induces a lowering of the AlF_4^- content as can be seen from Figure 6. In cryolite, the effect is almost negligible and increases with the acidity of the melt. For high CaF_2 additions (>15−20 mol %), some deformations of the AlF_5^{2-} band can be observed (broadening, shift of frequency). A detailed study of these spectra has been described in another paper,[13] and we will concentrate on the comparison between the Raman data and the vapor pressure results only. Since CaF_2 shifts equilibria 1 and 2 to the left, it means that it has to dissociate in some way to liberate F^-. On the other hand, vapor pressure shows that the activity of $NaAlF_4$, does not decrease, or decrease very little. This apparent contradiction can be explained.

Let us consider a mixture made up of $n^{\circ}_{AlF_3}$, n°_{NaF} and $n^{\circ}_{CaF_2}$ moles of AlF_3, NaF and CaF_2, respectively in such a way that $\sum n_i^{\circ} = 1$. The Raman spectrum of such a melt shows the relative distribution of AlF_4^-, AlF_5^{2-}, and AlF_6^{3-}, but not their anionic concentrations, since we have no indications from the spectra

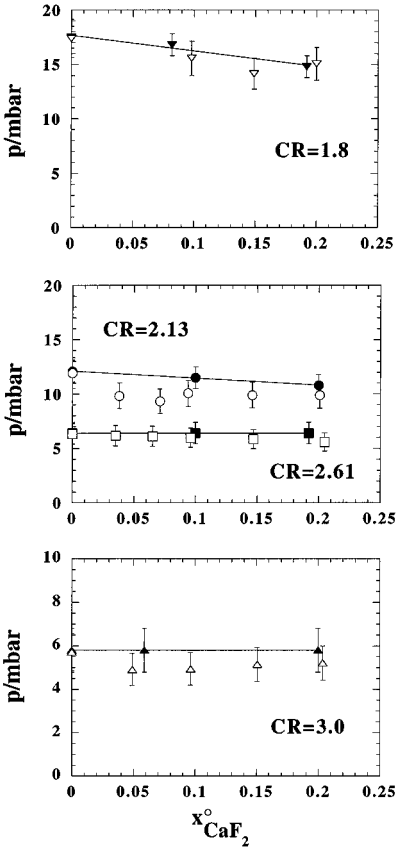

Figure 18. Experimental and calculated vapor pressures above NaF−AlF_3−CaF_2 melts at 1293 K. $CR = 1.78$ (1.8): (▼) observed; (▽) calculated. $CR = 2.13$: (●) observed; (○) calculated. $CR = 2.61$: (■) observed; (□) calculated. $CR = 3$: (▲) observed; (△) calculated.

on the amount of free F^- and Ca-containing species. The molar fraction of AlF_4^- is equal to $n_{AlF_4^-}/n^{\circ}$, where $n_{AlF_4^-}$ is the number of moles of AlF_4^- calculated from the spectra, and n° is the total number of mole of anions. Due to the CaF_2 addition, $n_{AlF_4^-}$, $n_{AlF_5^{2-}}$, and $n_{AlF_6^{3-}}$ decrease. Moreover, due to the observed shift of equilibria, $n_{AlF_4^-}$ decreases more than just due to dilution. However, since we do not know the value of n°, we do not know how $x_{AlF_4^-}$ will vary. For instance, when MgF_2 was added, reaction 20 indicated a reduction of n° that contributes to an increase in $x_{AlF_4^-}$. We therefore envisaged a model similar to the one proposed for MgF_2. This is supported by the observation of a deformation of the AlF_5^{2-} spectrum at high CaF_2 additions, even if this deformation is smaller than in the MgF_2 case. Moreover, the spectra of NaF−CaF_2 mixtures do not exhibit bands typical of any Ca-containing complex. These observations are understandable, since the bond between Ca^{2+} and F^- are much weaker than the bond between the smaller Mg^{2+} and F^-. Even the Mg−F bands do not give strong Raman effects. We will due to the above reason propose the reaction scheme given below for dissolution of CaF_2:

$$CaF_2 + (3 - n)AlF_5^{2-} = CaF_n(AlF_5)_{3-n}^{(4-n)-} + (2 - n)F^- \quad (21)$$

Here n varies from 2 to 0. When CaF_2 is dissolved according to this model, it associates with AlF_5^{2-}, forming mixed complexes, and F^- may be released. One can note that reaction 21 does not seem to change the number of anions. It is important to remember that the addition of CaF_2 does not produce additional cations in the melt. For a constant number of moles $\sum n_i^{\circ} = 1$, $n^{\circ}_{AlF_3}$ and n°_{NaF} will decrease when CaF_2 is added. The net effect is a decrease in the total number of moles of anions. This results in a more or less constant value of $x_{AlF_4^-}$.

Raman data have been obtained for the system $NaF-AlF_3-CaF_2$, for $CR = 1.78$, 2.2, 2.6, and 3, with various CaF_2 contents. As explained above, we can calculate the number of moles AlF_4^-, AlF_5^{2-}, and AlF_6^{3-} from the spectra and the scattering coefficients. It is then possible by using the model reaction 21 to calculate the anionic concentration of all the species.

Knowing the ionic distributions, vapor pressures can be calculated as outlined previously. The results obtained are compared with our measured vapor pressures in Figure 18. This comparison shows the following.

The agreement between vapor pressures calculated from Raman data and measured vapor pressure for ternary $NaF-AlF_3-CaF_2$ melts are quite satisfying if we consider the complexity of these melts.

The slope of p vs $x^\circ_{CaF_2}$ for low concentrations of CaF_2 is not exactly the same for measured and calculated pressures. However, if eq 21 is written as $CaF_2 + nAlF_5^{2-} \rightarrow CaF_2(AlF_5)_n^{2n-}$, the same limiting slopes would be obtained for $n = 1.8$. To fit the model to the measured pressures, n should vary from 1.8 to 1 for increasing CaF_2 contents. This is not very surprising since for small additions, CaF_2 may be solvated more easily.

Concluding Remarks

Quantitative Raman is a powerful tool in the analysis of structure of molten salts, and may also be of importance for the characterization of the technical Al−electrolyte.

A combination of quantitative Raman and thermodynamic data gives new insight into the structure of complex salt mixtures.

The structure of cryolitic melts is much more complex than previously anticipated. The models suggested in the present paper may also be less general than indicated. When the MF_2 salt added to the $NaF-AlF_3$ binary is more basic than MgF_2 and CaF_2, a new cation may be formed and the stoichiometric equilibrium constants for the two anion equilibria observed from the Raman data have to vary with the MF_2 concentration. We will come back to this problem in a forthcomming paper.

Acknowledgment. This project has benefitted scientifically and financially from our participation in a Human Capital and Mobility Network of the European Communities. Financial support from The Research Council of Norway and the Norwegian aluminium industry is also gratefully acknowledged. The FNRS of Belgium is acknowledged for financial support to E.R. We will also express our thanks to Ernest Dewing for pointing out some errors in our interpretation of the acid−base behavior of CaF_2 in cryolitic melts presented in our paper in Light Metals 1995.

Supporting Information Available: Tables of vapor pressure data for the $NaF-AlF_3-MF_2$ (M = Ca and Mg) systems available as log $p_{tot}/mbar = A - 10^{-3}B/T$ (K), mole fractions of anions given for the $NaF-AlF_3$ binary system as a function of composition and temperature, and the number of moles of AlF_4^-, AlF_5^{2-}, and AlF_6^{3-} given for the $NaF-AlF_3-MF_2$ (M = Ca and Mg) melts for $T/K = 1293$ (MgF_2) and $T/K = 1273$ and 1293 (CaF_2) (5 pages). Ordering information is given on any current masthead page.

IC951660L